THE EFFECT OF AIR-SIDE LEAKAGE IN ROLL WINDING

by

H. Lei and K. A. Cole
Eastman Kodak Company
USA

ABSTRACT

In web winding processes, a thin layer of air is entrained into rolls during winding. This air reduces the interlayer pressure in the wound roll because the air acts like a sponge between adjacent web layers. Winding models that include the effect of air entrainment have been developed in recent years to provide better prediction of wound-roll stresses and wound-roll quality. However, these models have limited predictive success in narrow-web winding, especially when a pressure roller is not used. During winding, and after a roll is wound, the air in the roll leaks out of the sidewalls through narrow gaps between the layers. The amount of air leaking through the sidewall, when the web is narrow and has a rough surface, is significant. When side leakage is not properly considered, the accuracy of the air entrainment model can be greatly affected. In this paper, a new winding model is developed that includes the effects of air entrained during winding and the subsequent air leakage through the sidewalls during and after winding. The formulation considers the effects of both pressure-roller and nonpressure-roller winding. Some results of this model are presented, together with comparisons to experimental results and predictions from other historical models (e.g., nonair entrainment and air entrainment without side leakage).

NOMENCLATURE

ε	strain
μ	air viscosity
ν	Poisson's ratio
ca	air film clearance between layers
ca_0	reference air film clearance
ca_w	air film clearance under the outer lap
ca_{w0}	air film clearance under winding nip
cc_0	reference contact clearance
cc_w	contact clearance under the outer lap

cc_{w0}	contact clearance under winding nip
E	web modulus
E_c	core modulus
$f(cc_w)$	contact pressure at contact clearance cc_w
h_c	thickness from one layer to the next in a roll
P	pressure in roll
p_a	ambient air pressure
p_g	local air gage pressure
p_g'	local air gage pressure under outer lap
p_{g0}'	air gage pressure under winding nip
r_d	radius of the winding roll
T	tension stress in roll
t	time
t_a	wound-in tension
V	winding speed
x	widthwise location

INTRODUCTION

Proper in-roll stresses after webs are wound onto a core are critical to the roll integrity and the web quality. High in-roll pressure is a major source of waste due to core impressions, hardstreaks/ridges, and core crush. Low in-roll pressure, conversely, is a major source of in-roll cinching, telescoping, dishing, loose core, and gapping.

Because of this strong correlation between in-roll stresses and the roll/web quality, researchers have developed many theoretical models to predict how the roll winding process settings can change the in-roll stresses. Altmann [1] was among the first to develop models that treat a winding roll as a linear orthotropic elastic medium. Later, Hakiel [2] extended Altmann's model to include a nonlinear constitutive relation that characterizes the stack modulus. Hakiel's model has been very successful in predicting the in-roll stresses at low-speed windings, especially when the webs are narrow. At high-speed windings, experiments by Good and Holmberg [3] have indicated that the in-roll stresses and wound-roll integrity decrease as speed increases. At higher speeds, more air is entrained into the roll during winding, and the air acts as a cushion that lowers the stack modulus and stresses. To obtain the same wound-roll quality at an increased winding speed, the most common approaches are winding rolls with higher tension and/or adding a pressure roller to reduce the air entrainment. Winding models that incorporate the effect of air entrainment include those by Good and Holmberg [3], Forrest [4,5], Bourgin [6], and Lei and Cole [7]. These air-entrainment winding models have been successful in predicting in-roll stresses in high-speed winding of wide webs, especially when a pressure roller is used. However, their predictions on narrow-web center winding have been less successful.

During winding, the air in the roll leaks out through the sidewalls because of the air pressure difference in the roll and in the ambient air. Leaking air from sidewalls offsets the effect of entraining air to winding. Air leaking effect is especially obvious during winding of a narrow web that has a rough surface, when the air leaking is a significant

percentage of the total air entrained at the winding nip. In that case, a typical air entrainment model, without considering air leakage effect, under-predicts the in-roll pressure. Conversely, when winding a wide web that has a very smooth surface, the air leaking through the sidewalls is slow and negligible in the timeframe of interest, and the air entrainment model without side leakage predicts more reasonable results. In between the above extremes, a winding model that includes both air entrainment and air side-leakage effects is necessary to accurately predict the wound-roll stresses. Figure 1 describes how different models can be applied in the winding of different webs with varying width and roughness.

After a roll is wound, more air in the roll leaks, and the stresses reduce further. The stress "relaxation," due to air leakage after winding, behaves similarly to the stress relaxation that occurs when rolls are stored at high temperatures.

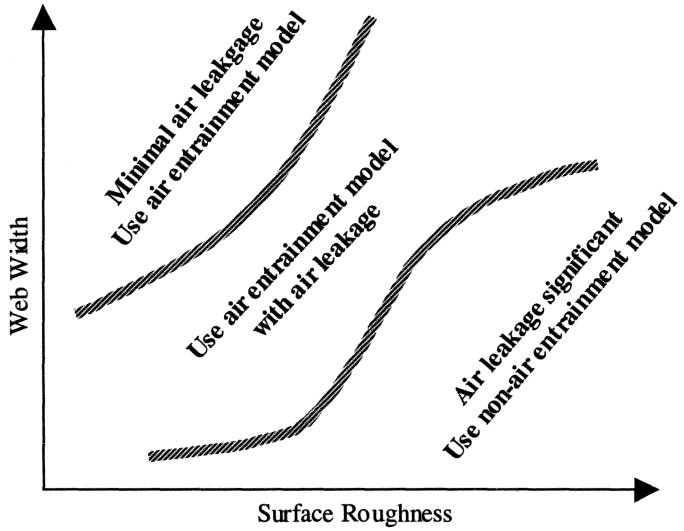

Figure 1 – The schematic drawing of the validation of models for winding of webs with different width and roughness.

The objective of this paper is to incorporate the effect of air side-leakage into the air entrainment winding model. Some results of this model will be presented, together with comparisons to experimental results and predictions from other historical models (e.g., nonair entrainment and air entrainment without side leakage).

AIR-LEAKAGE WINDING MODEL

In this section, we develop an analysis that describes the air leakage through the edges of the roll, and incorporate the analysis into the air-entrainment winding model. The model consists of an analysis under the outer lap and an analysis within the winding roll.

Air leakage through the edges of the roll

To simplify the analysis and avoid the complication of including the shell bending across the width, the following assumptions are made in the development of the air-leakage winding model.

1) Only the winding of an ideal web is considered—web thickness and wound-roll geometry are assumed uniform across the width. The layer-to-layer gap clearance is also assumed invariant across the width. The in-roll air pressure, however, can vary along its widthwise location. To satisfy the force equilibrium requirement, the total radial in-roll pressure is balanced by the contact pressure through the rough support, between the contacting surfaces, and the average of air pressure across the width.
2) In the winding/wound roll, the air movement relative to the web along the machine direction is neglected. This assumption is reasonable considering that the roll length is often significantly larger than the web width, the air pressure gradient along the length direction is far less than that of the cross width direction, and cross width direction has two edges which are exposed to the ambient air.

With the above assumptions, the air gage pressure (the pressure above the ambient pressure) on the widthwise direction in a winding/wound roll can be described by the squeeze-film equation [8]

$$\frac{\partial^2 p_g}{\partial x^2}+\frac{1}{p_g+p_a}\left(\frac{\partial p_g}{\partial x}\right)^2=\frac{12\mu}{ca^3}\left(\frac{ca}{p_g+p_a}\frac{\partial p_g}{\partial t}+\frac{\partial ca}{\partial t}\right), \qquad \{1\}$$

where p_g is the local air gauge pressure which varies along the widthwise location x, p_a is the ambient pressure, ca is the air-gap clearance between the layers, μ is air viscosity, and t is the time. In arriving at Equation {1}, we have assumed the effect of slip boundary between the air molecules and the wall is negligible, the air follows ideal gas law, the flow between the layers is laminar, and the web surface roughness has no impedimental effect on airflow.

The boundary conditions for the air gage pressure are those at the edges, the air pressure reaches the ambient pressure

$$p_g=0 \text{ at } x=0 \text{ and } x=w, \qquad \{2\}$$

w being the width of the web.

In the following sections, equation {1} is coupled with the roll winding analysis to describe the air entrainment, air leakage, and their interactions with the in-roll stresses.

Outer-lap analysis

Under the outer lap, the total pressure from the winding tension is balanced by the summation of the air gage pressure arising from the entrained air, and the contact pressure from the direct contact between the rough surfaces. Using the treatments of the web roughness model and the relation between the contact pressure and the contact clearance [7], the force balance under the outer lap becomes

$$\frac{t_a}{wr_d} = ave(p_g') + f(cc_w), \qquad \{3\}$$

where t_a is the wound-in tension, cc_w is the contact clearance under the outer lap, and r_d is the radius of the winding roll. In equation {3}, $f(cc_w)$ is the contact pressure that relates to the contact clearance, the relation of which can be derived from the stack modulus measurements. For center winding without an idling pressure roller, the wound-in tension is the same as the machine tension just upstream of the winder. For center winding with the assistance of a pressure roller, the wound-in tension includes both the machine tension and the nip-induced tension. The air gage pressure is p_g', and it varies across the width. During the winding of this outer lap, the air leaks out of the sidewall simultaneously, and, therefore, the air gage pressure, p_g' and cc_w, can vary circumferentially under this outer lap. However, equation {3} still holds locally under the outer lap, if we assume the wound-in tension loss due to the friction between the outer lap and the wound roll is negligible.

Air entrainment in a center winding without idling pressure roller. For a center winding without the assistance of an idling pressure roller, prior to the addition of a new lap, the roll has radius r_d. While adding this new lap, the air gage pressure at the entrance nip is related to its air clearance, ca_{w0}, using the foil-bearing equation [8]

$$p_{g0}' = \frac{12\mu V}{r_d}\left[\frac{0.643 r_d}{ca_{w0}}\right]^{3/2} \qquad \{4\}$$

where V is the winding speed, ca_{w0} is the air film clearance that corresponds to the contact clearance cc_{w0} at the entering nip. They are related by

$$cc_{w0} - ca_{w0} = cc_0 - ca_0, \qquad \{5\}$$

where cc_0 is the reference contact clearance, and ca_0 is the reference air film clearance [8].

Air entrainment in a center winding with idling pressure roller. The addition of a pressure roller to the center winding significantly reduces the amount of air entrainment into the roll. In this paper, the amount of air entrainment into the winding nip is estimated by the same pressure roller nip analysis as detailed in Chang [9], and used by Lei and Cole [7]. From the pressure roller nip analysis, the air pressure entering the nip, p_{g0}', and the initial contact clearance after the nip, cc_{w0}, are available.

Coupling of air leakage to the outer lap analysis. Once passing the winding nip, the air leakage from the edges under the outer lap can be significant, especially for narrow webs that have rough surfaces. In the following analysis, the winding of the outer lap is simplified to a process described in Figure 2. The values of air gage pressure and contact clearance at the entering nip, p_{g0}' and cc_{w0}, are available by solving equations {3,4}. From the entering nip to the end of the outer lap, the air leakage from edges is described by the squeeze-film equation {1}. The time needed to wind the outer lap is $2\pi r_d / V$. Within this time period, the air pressure and the contact clearance exiting the outer lap, p_g' and cc_w, are available by solving equations {1,3}. The results are used in the in-roll analysis that follows.

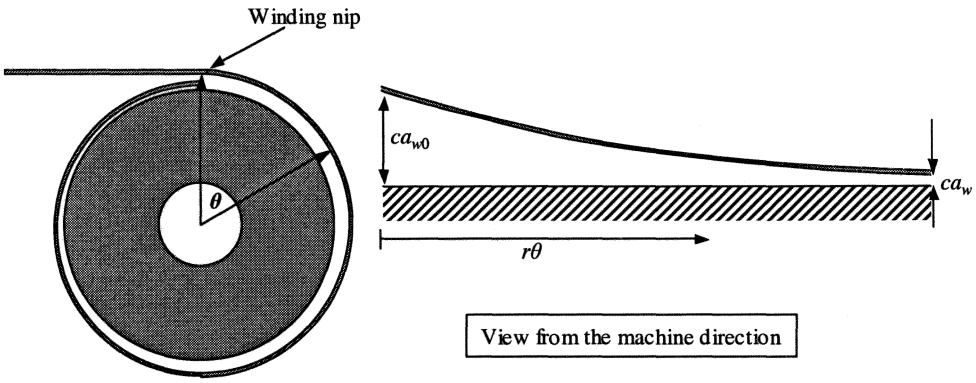

Figure 2 – The air leakage through the sidewalls, under the outer lap.

In-Roll Analysis

In a winding/wound roll, the air leaks under each lap, and in theory the air pressure would change circumferentially. In this analysis, we follow the idealization of most traditional models and assume the roll is made up of individual laps (hoops), shrunk fit one on top of the other. The pressures under each lap are assumed not varying circumferentially, but they can vary from one lap to another.

Under each lap within a winding/wound roll, the axial air movement through the narrow channels between the layers can be described by the squeeze-film equation {1}. In-roll stress changes as more laps are added onto the winding roll. Additionally, the in-roll stress changes as the air leaks out from the sidewalls. Figure 3 illustrates how the stress changes, due to the leaking air, can be described in theory. At time t, in a winding/wound roll the pressure is P^0, in-roll tension is T^0, and, under the stresses, the radial strain is ε_r^0 and tangential strain is ε_θ^0; all are functions of radial location. After part of the air in the roll leaks out (time $t + \Delta t$, Δt being the an infinitesimal time step), the in-roll stresses change to pressure $P^0 + \Delta P$, tension $T^0 + \Delta T$, and the strains in the roll become radial strain, $\varepsilon_r^0 + \Delta\varepsilon_r^f$, and tangential strain, $\varepsilon_\theta^0 + \Delta\varepsilon_\theta^f$. The total change in strain (deformation gradient to be more precise) in the winding/wound roll during this infinitesimal time period, Δt, can be decomposed into two individual steps [10], as shown schematically in Figure 3:

1. Change in strain due to air leakage, and

2. Change in strain due to mechanical deformation afterwards.

The change in strain due to the air leakage (step 1) transforms the roll from the initially equilibrium state (at time t) to an intermediate imaginary state, which is not necessarily in mechanical equilibrium. There is no web physical movement during step 1. Following step 1, the change in strain due to the mechanical equilibrium (step 2) deforms this imaginary state to its equilibrated state, the state at time $t + \Delta t$. As the air leaks out during step 1, the in-roll strain shifts, the in-roll pressure drops to P^*, and the radial strain changes $\Delta\varepsilon_r$. Since web doesn't physically move during step 1, the circumferential strain and stress stay the same. In the state after air leakage and mechanical deformation (Figure 3 (c)), the wound roll reaches mechanical equilibrium. At this final equilibrated state (Figure 3 (c)), the in-roll pressure is $P^0 + \Delta P$, the tangential stress becomes $T^0 + \Delta T$, and strains are $\varepsilon_r^0 + \Delta\varepsilon_r^f$ and $\varepsilon_\theta^0 + \Delta\varepsilon_\theta^f$. In the above, $\Delta\varepsilon_r^f$ includes change in strain due to air leakage $\Delta\varepsilon_r$ and the change in strain due to the re-establishment of mechanical equilibrium (from state (b) to state (c)). Conversely, $\Delta\varepsilon_\theta^f$ includes only the change in circumferential strain from the re-establishment of mechanical equilibrium.

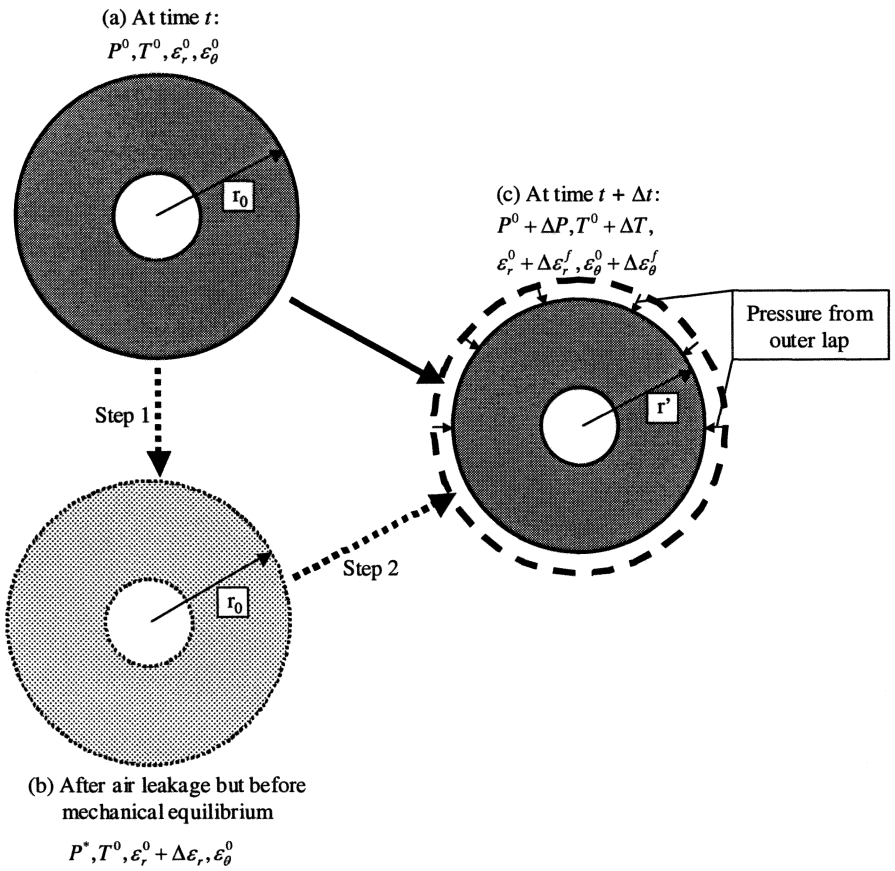

Figure 3 – The effect of air leakage to the wound-roll stresses.

The equilibrium of the winding/wound roll after air leakage requires that

$$\Delta P + \Delta T + r\frac{d\Delta P}{dr} = 0 \quad . \qquad \{6\}$$

Constitutive relation of the wound roll requires that

$$\Delta\varepsilon_\theta^f = \frac{\Delta T}{E_x} + \frac{\nu_{\theta r}}{E_{ya}}\Delta P \quad , \qquad \{7\}$$

$$\Delta\varepsilon_r^f = -\frac{\nu_{r\theta}}{E_x}\Delta T - \frac{\Delta P}{E_{ya}} \quad . \qquad \{8\}$$

where $\nu_{r\theta}$ and $\nu_{\theta r}$ are the two components of Poisson's ratio relating strain in one direction to strain in the other, E_x is the Young's modulus along the circumferential direction, and E_{ya} is the stack modulus including the effect of remaining air between layers [7]. Conversely, the change in strain due to the re-establishment of mechanical equilibrium must satisfy kinematic relationships between the strain and deformation,

$$\Delta\varepsilon_\theta^f - \Delta\varepsilon_r = \frac{dU_{II}}{dr} \quad , \qquad \{9\}$$

$$\Delta\varepsilon_r^f = \frac{U_{II}}{r} \quad , \qquad \{10\}$$

where U_{II} is the radial displacement during the mechanical deformation (from state (b) to state (c)) after air leakage. Equations {9, 10} reduce to the compatibility equation of the strain

$$r\frac{d\Delta\varepsilon_\theta^f}{dr} + \Delta\varepsilon_\theta^f - \Delta\varepsilon_r^f + \Delta\varepsilon_r = 0. \qquad \{11\}$$

When using the constraint on Poisson's ratio [2]

$$\frac{\nu_{\theta r}}{E_{ya}} = \frac{\nu_{r\theta}}{E_x} \quad , \qquad \{12\}$$

the equations above are reduced to a second order ordinary differential equation that governs the change in the in-roll pressure from the air leakage and/or the adding of a new lap in a winding/wound roll

$$r^2\frac{d^2\Delta P}{dr^2} + 3r\frac{d\Delta P}{dr} + \left(1 - \frac{E_x}{E_{ya}}\right)\Delta P = E_x\Delta\varepsilon_r \quad . \qquad \{13\}$$

Boundary conditions for the above differential equation are that

- At the core/roll interface

$$\frac{d\Delta P}{dr} = \frac{2}{c}\left(\frac{E_x}{E_c} - 1 + \nu_{r\theta}\right)\Delta P \quad . \qquad \{14\}$$

- At the outside periphery of the roll

$$\Delta P = \begin{cases} \dfrac{t_a(i)}{wr(i)} & \text{for a winding roll} \\ 0 & \text{for a wound roll} \end{cases} \quad . \qquad \{15\}$$

In the above equations, total pressure change ΔP consists of the change in the contact pressure ΔP_c and the change in the air pressure between the neighboring layers. The latter is given as the average of air gage pressure over the whole width. Therefore,

$$\Delta P = \Delta P_c + ave(\Delta P_g) \quad . \qquad \{16\}$$

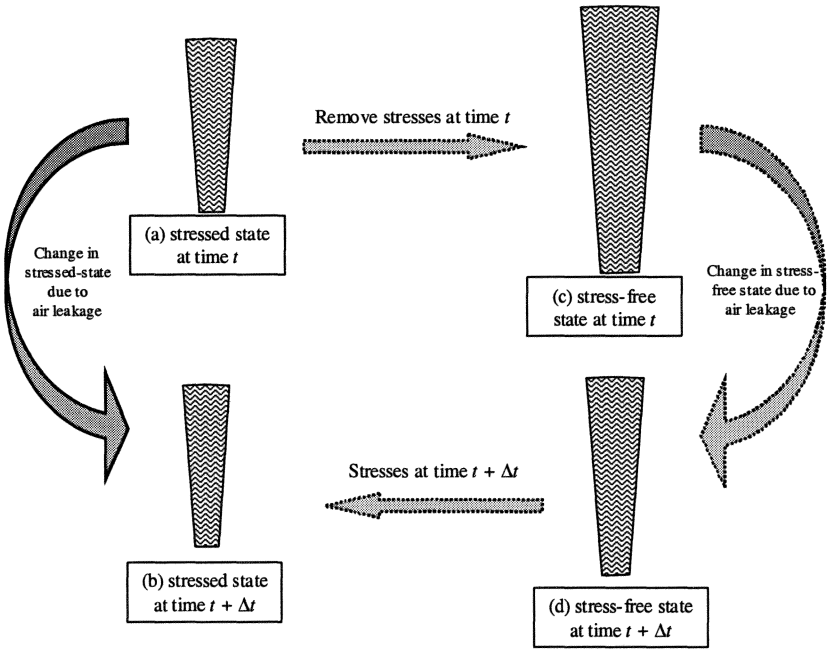

Figure 4 – The schematic diagram of the stress-free states.

In equation {13}, $\Delta\varepsilon_r$ is the change in local radial strain due to the air leakage from the sidewalls and, therefore, its value should correlate to the amount of air leaking out. To derive this correlation, we consider a radial element taken out of a

winding/wound roll (Figure 4). The air leakage during the infinitesimal time step Δt transforms this element from the stressed state (a) to a new stressed state (b). Again, similar to the analysis by Lee [10], the changed from (a) to (b) in Figure 4 can be decomposed into the following steps:

1. Removing stresses in state (a) at time t to get its stress-free state (c),
2. Changing stress-free state (c) to stress-free state (d) as the air leaks out,
3. Adding stresses back to state (d) to arrive the new stressed-state (b).

From t to $t + \Delta t$, the change in strain primarily comes from the change in the gap clearance as the air leaks out. Therefore, the change in radial strain can be approximated as

$$\Delta\varepsilon_r \approx -\frac{\Delta cc_{wc}}{h_c} \quad , \qquad \{17\}$$

where h_c is the local lap thickness from one layer to the next, cc_{wc} is the contact clearance in a stress-free state, and Δcc_{wc} is the change in cc_{wc} from t to time $t + \Delta t$. At the stress-free state (c) or (d), the equations governing stress-free contact clearance cc_{wc} and its corresponding average air pressure across the width $ave(P_{gc}^{"})$ are

$$ave(P_{gc}^{"}) + f_{(cc_{wc})} = 0 \qquad \{18\}$$

$$\left(ave(P_{gc}^{"}) + P_a\right)\left(cc_{wc} - cc_0 + ca_0\right) = \left(ave(P_g) + P_a\right)\left(cc - cc_0 + ca_0\right) \qquad \{19\}$$

where P_g is the air gage pressure in the winding/wound roll. Equation {18} simply states that in the stress-free state, the sum of air gage pressure (averaged over the width) and the contact pressure should vanish to satisfy a stress-free state. Equation {19} is the requirement of the air mass balance.

NUMERICAL IMPLEMENTATION

The numerical implementation of the above model starts with the outer lap analysis of each winding lap, which evaluates the amount of air entrapped through the winding nip [7]. Next under the outer lap, equations {1,3} are coupled to solve for the air pressure and the contact clearance exiting the outer lap (or the entrance to the existing roll). The results are used in the in-roll analysis. The program follows the following steps:

1. Wind one lap; evaluate the amount of air entrapped under the winding nip. Solve {1,3} for the air pressure and contact clearance exiting the outer lap.
2. Equations {1,13-19} are solved for the in-roll stresses and air gap after the addition of this new lap and also the air gage pressure after this new lap is wound.
3. Update pressure, tension, web reference thickness, etc.

4. Evaluate strain due to air leakage.
5. Repeat steps 2-4 until the solution is converged.
6. Repeat steps 1-6 until all laps are wound.
7. Solve equations {1,13-19} for the in-roll stress distribution after winding.

RESULTS AND DISCUSSION

Experiments and model predictions

A big roll of silver-halide, –emulsion-coated photographic paper is slit and wound into small rolls at 450 m/min (500 m length each). Slit rolls are each 10.16 cm (4 in.) wide, and are wound onto cardboard cores (8.71 cm OD). The individual winders on the slitter are independently driven. Each small roll is wound with a tension starting at 91.4 N (5.14 pli), and the tension tapers linearly with roll length to 73.1 N (4.11 pli) at the end of the 500 m. No pressure roller is used in the operation. After winding, the slit rolls are tested for their telescoping forces (the forces that make the rolls shift) using a roll telescoping force gauge (Figure 5). The roll telescoping force is divided by the roll circumferential area and the web front-to-back coefficient of friction (0.46, based on Capstain friction tests; same value used for the coefficient of friction between the web and the core) to arrive at the in-roll contact pressure. The results of the in-roll contact pressure at different radial locations, together with their 95% confidence limits, are shown in Figure 6.

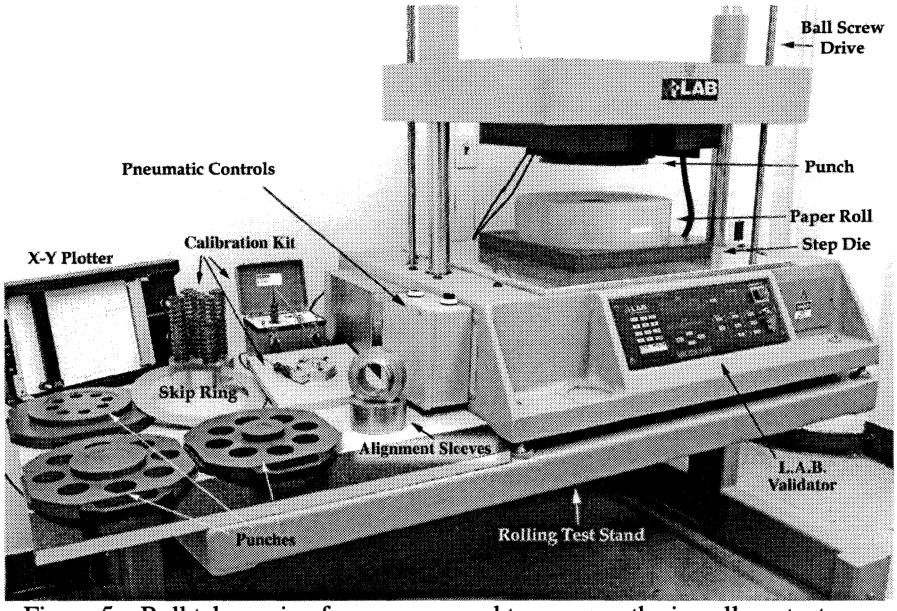

Figure 5 – Roll telescoping force gauge used to measure the in-roll contact pressure at different radial locations.

Also shown in Figure 6 are predictions from the current winding model, together with other models. When a traditional winding model, excluding the air entrainment [2], is applied to the same conditions, the model over predicts the in-roll pressure by a factor of approximately 2. The difference is generally due to the entrained air, which acts like a sponge between the layers. Figure 6 also shows the contact pressure predictions from a

winding model that considers the effect of air entrainment but excludes air leakage. Apparently, when air leakage through the sidewalls is excluded, the air entrainment model under predicts the in-roll contact pressure. This air entrainment model even falsely predicts, at certain stages during winding, that the laps will start floating (no physical contact between neighboring laps), and in-roll pressure is solely supported by air between the layers. The current model, which includes both air entrainment effect and air side-leakage effect, is more reasonable and predicts an in-roll pressure between the traditional model and the air-entrainment model without air leakage.

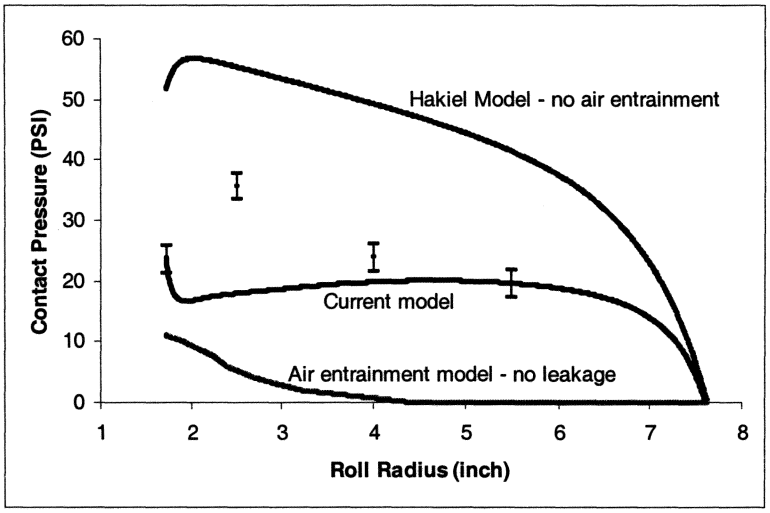

Figure 6 – Predictions of the in-roll pressure from different models and their comparison to the experimental data.

The parameters used in the above models are listed in Tables 1 and 2. The reference contact clearance and air film clearance in Table 1 are determined from Wyko surface roughness measurements of both the front and the backside of the web. The root-mean square of the front and backside peak-to-valley surface roughness is used as the reference contact clearance cc_0, and the root-mean square of the engagement heights of the front and backside surfaces [11] is used as an approximation of the air film reference clearance ca_0.

Table 1: Material properties used in the winding models.

Core OD, cm	8.71	E_x, MPa	5720
Web Thickness, um	223.98	Bulk Modulus E_s, MPa	179
cc_0, um	6.57	E_c, MPa	391
ca_0, um	5.44	Poisson's Ratio	0.02

The air leakage model provides a tool that is capable of predicting the dynamic change in pressure, air gap, amount of air in the roll, and others. For the winding of the paper slit rolls above, Figure 7 shows the predictions of air gage pressures (the air pressure above the ambient air) and the gaps (contact clearance) under the 1st lap (the gap between the roll and the core), and under the 300th lap. From the predictions, the air

pressure increases in the beginning due to the addition of more laps and, simultaneously, contact clearance decreases. However, the air pressure starts to drop after a certain number of laps is added, generally because the leaking of air from the sidewalls. At the winding of the 300th lap, the tension is lower than the starting tension, which is due to its tapering tension profile, and the roll diameter is larger than the core diameter. Based on the foil-bearing theory, lower tension and larger roll diameter exacerbate the amount of air entrainment and, thus, resulting in a lower air gage pressure and a higher initial contact clearance, as shown in Figure 7. After winding the 200th lap, the gap clearance under the 1st lap approaches its final value, and the air gage pressure approaches a zero value, which is in equilibrium to the ambient air.

Table 2: Roughness modulus of the silver-halide emulsion coated paper.

Contact Clearance, um	Contact Pressure, Mpa	Stack Modulus, MPa
6.57	0.000	0.022
4.42	0.014	0.085
3.72	0.028	0.186
3.34	0.041	0.293
2.23	0.138	1.038
1.42	0.345	2.721
0.84	0.689	5.548
0.31	1.379	12.473
0.02	2.413	43.147

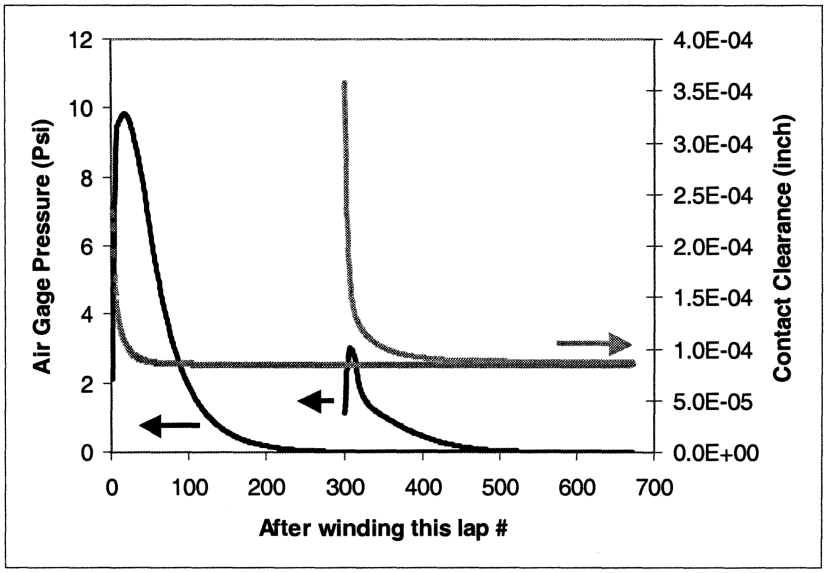

Figure 7 – Air pressure and contact clearance under the 1st and the 300th laps during winding.

As more laps are wound onto the roll, the pressure in the roll increases, and the gap clearance decreases. During winding, the amount of air remaining under the 1st lap (the gap between the roll and the core) is plotted against the winding lap number in Figure 8. It shows that in the gap between the 1st lap and the core, half of the air leakage takes

places before winding of the 10th lap, and 90% of the air leakage takes place before winding of the 58th lap, which is only very small portions of the roll winding process; the whole roll consists of winding 671 laps.

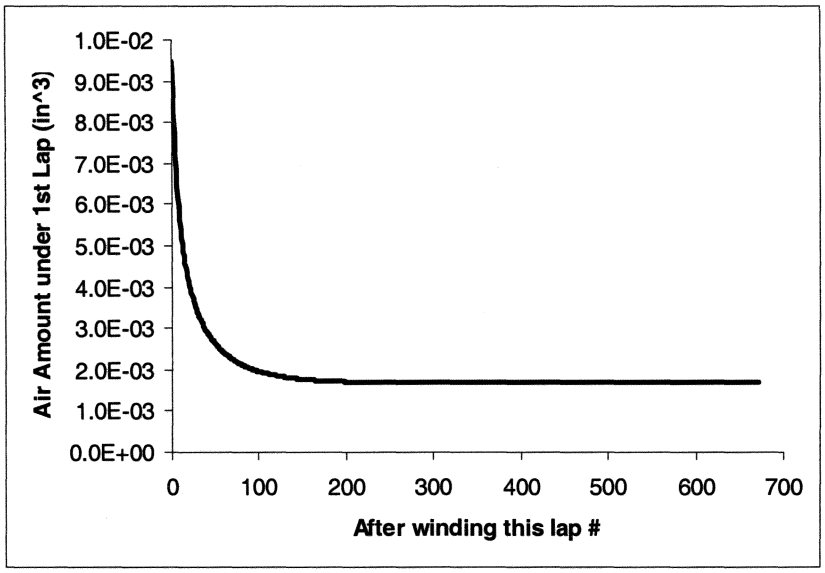

Figure 8 – The amount of air (adjusted to ambient air pressure) left under 1st lap during winding.

Web width effect during winding

Web width of a winding roll significantly affects the time needed for the air between layers to leak out. Simple dimensional analysis on the squeeze film equation {1} reveals that the characteristic air leaking time τ is

$$\tau = \frac{12\mu w^2}{p_{atm} cc^2} \quad , \qquad \{20\}$$

where cc is the typical air gap between the layers. This shows that the time required for the air to leak out is proportional to the width square and inversely proportional to the gap clearance square. Doubling the web width or reducing the surface roughness by half, the time required for air to leak out is quadrupled. As a result, when rolls with different widths are wound at the same speed and tension per width, they could have significantly different in-roll pressure and wound-roll quality. Figure 9 shows the model predictions of this width affect on contact pressure right after roll winding. The parameters used in the predictions are the same as those in Table 1 and 2, except the width is varying. For comparison purposes, Figure 9 also includes model predictions from the traditional model without air entrainment [2], and the air entrainment model excluding air leaking [7], both of which predict width-independent results. The current model predicts that, as the web width decreases, the in-roll contact pressure increases because of the fact that air is leaking faster from the sidewalls, so the air in-roll has less affect on the winding. Theoretically, as the web width approaches zero, the air entrained into the roll immediately leaks out from the sidewalls and, thus, the air would not have any impact on

winding. In that scenario, the air leakage model prediction would match the traditional model prediction. Conversely, when the web gets wider, the air needs more time to leak out, and the in-roll contact pressure will drop because more air stays in the roll during winding. Again in theory, if the web approaches infinitely wide, the air leakage would no longer have any impact on winding and, thus, the air leakage-model prediction should match the prediction from the air entrainment model without air leakage effect.

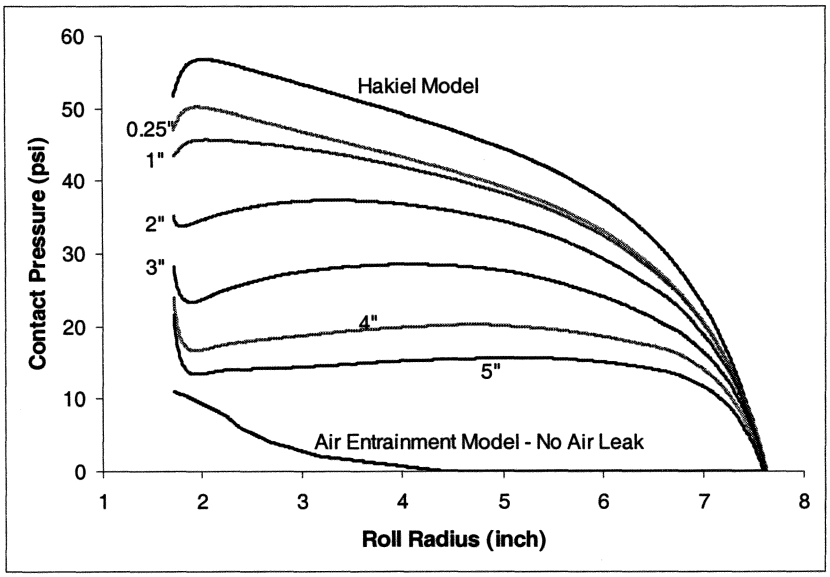

Figure 9 – Web width effect during winding.

Sensitivity to the reference air film clearance

In the air entrainment model presented here and by Lei and Cole [7], the reference air film clearance, ca_0, is defined as the average of void space (gap) between two surfaces (web front and back surfaces) at the incipient contact conditions. In the examples shown so far in this article, the root-mean square of the engagement heights from the Wyko surface roughness measurement is used as the air film contact clearance. The approximation of the engagement height as the reference contact clearance is appropriate for webs like typical papers and polyester films whose surface roughness peak height is close to a Gaussian distribution. However, the above approximation of the reference air film clearance is not appropriate for webs with non-Gaussian peak height distribution, e.g., when mat beads are added to the surface. In the winding of the paper rolls above, the model predictions are relatively sensitive to the model input of the reference air film clearance. Figure 10 shows the results of the in-roll contact pressure in the wound roll at 6 levels of reference air-film clearances, ranging from 60% to 100% of the reference contact clearance, cc_0. At lower values of the reference air film clearance, the entrapped air needs more time to leak out from the roll sidewalls, and the in-roll contact pressure is lower.

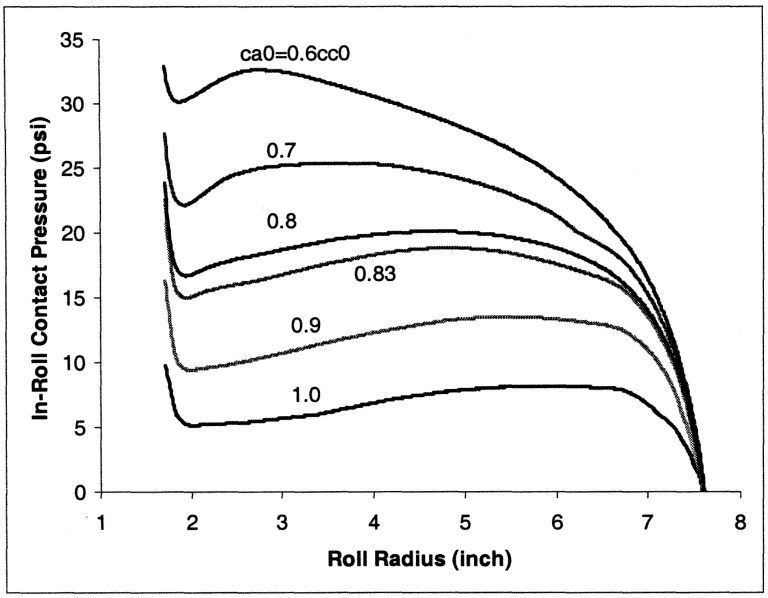

Figure 10 – The sensitivity of reference contact clearance to the model prediction.

SUMMARY

A theory is developed to describe the air leaking from the sidewalls of a winding/wound roll. This theory is coupled with the air entrainment-winding model to predict the effect of leaking air to the wound-roll stresses and wound-roll quality. This new model provides a capable tool of tracking the amount of air left in a winding/wound roll. It predicts that, in addition to winding tension, pressure roller force, and winding speed, web roughness and web width also affect the stresses in the roll. The current model predictions are compared to experimental results and, also, other winding model predictions. The comparison shows that the current model gives a more reasonable prediction in the wound-roll stresses than other models. The width effect of the winding web to the wound-roll stresses is studied, and the sensitivity of this model on the model input of reference air-film clearance is discussed.

ACKNOWLEDGMENT

The authors thank J. W. Wysokowski of Eastman Kodak Company for providing the experimental data, and the photo illustrating the roll telescoping force gauge.

REFERENCES

1. Altmann, H.C., "Formulas for Computing the Stresses in Center Wound Rolls," Tappi Journal, Vol. 51, No. 4, 1968, pp. 176–179.
2. Hakiel, Z., "Nonlinear Model for Wound Roll Stresses," Tappi Journal, Vol. 70, No. 5, May 1987, pp. 113–117.
3. Good, J.K. and Holmberg, M.W., "The Effect of Air Entrainment in Centerwound Rolls, "Proceedings of the Second International Conference on Web Handling, Web Handling Research Center, Stillwater, OK, June 6–9, 1993.

4. Forrest, A.W., "Air Entrainment During Film Winding With Layon Rolls," Proceedings of the Third International Conference on Web Handling, Web Handling Research Center, Stillwater, OK, June 18–21, 1995.
5. Forrest, A.W., "Wound Roll Stress Analysis Including Air Entrainment and the Formation of Roll Defects," Proceedings of the Third International Conference on Web Handling, Web Handling Research Center, Stillwater, OK, June 18–21, 1995.
6. Bourgin, P., "Air Entrainment in Web Handling: To be Avoided or Mastered?" Proceedings of the Fourth International Conference on Web Handling, Web Handling Research Center, Stillwater, OK, June 1–4, 1997.
7. Lei, H. and Cole, K. A., "A Thermoelastic Winding Model with Air Entrainment," Proceedings of the Sixth International Conference on Web Handling, Web Handling Research Center, Stillwater, OK, June 10–13, 2001.
8. Gross, W. A., "Fluid Film Lubrication," John Wiley & Sons, New York, 1980.
9. Chang, Y.B., Chambers, F.W., and Shelton, J.J., "Elastohydrodynamic Lubrication of Air-Lubricated Rollers," ASME Journal of Tribology, Vol. 118, July 1996, pp. 623–628.
10. Lee, E. H., "Elastic-Plastic Deformation at Finite Strains", Journal of Applied Mechanics, Vol. 91, 1969, pp. 1–6.
11. Rice, B. S., Cole, K. A., and Müftü, S., "A Model for Determining the Asperity Engagement Height in Relation to Web Traction over Non-Vented Rollers," Transactions of the ASME, Vol. 124, July 2002, pp. 584–594.